Improved Matrix Synthesis for Inline Filters with Transmission Zeros Generated by FVC

Yong-Liang Zhang[1, 2, *]

Abstract—An improved matrix synthesis approach for inline filter is presented in this paper. Frequency-variant couplings (FVC) can generate and control multiple finite transmission zeros (TZs). As the resultant network only involves resonators cascaded one by one without any auxiliary elements (such as cross-coupled or extracted-pole structures), this paper provides the best optimizatised synthesis solution in configuration simplicity for narrowband filters based on genetic algorithm (GA) and solvopt optimization method. Compared with the conventional synthesis method for inline topology filters, the method presented in this paper has following advantages: First, it is unnecessary to consider both the couplings and capacitances of a traditional low-pass prototype. Second, there is no need to use similar transformation, and the adjacent FVCs can be implemented. Third, the approach presented can implement more TZs than the previous works. The maximum number of TZs can be as many as the filter order. Two examples with different topologies and specifications are synthesized to show the validation of the method presented in this paper.

1. INTRODUCTION

Implementing finite transmission zeros is crucial in the modern microwave filter design for the distinct improvement of out-of-band frequency selectivity. So over the past few decades, plenty of efforts have been made for the direct synthesis of narrowband microwave filters [1–11]. Basically, two topological configurations, namely cross-coupled [1–6] and extracted-pole [7–11], are introduced to generate the finite transmission zeros (TZs). The cross-coupled topology is widely applied for its ability of realizing all kinds of TZs (i.e., real, imaginary, and complex). However, tuning of filters with this topology may be quite inconvenient, since locations of the TZs are not independently tunable by a single element of the network. On the other hand, the extracted-pole topology allows TZs generated and tuned in an independent manner but suffers from the shortcoming that only imaginary TZs are realizable.

To take advantage of the configuration simplicity, a new concept of in-line topology filters has been recommended in recent years [12–20]. In [12, 13], an in-line configuration is produced by carefully implementing the bypass couplings between nonadjacent resonators (via the change of orientation for selected resonators). As these works are still based on cross-coupled topologies, the design complexity remains unchanged, and the TZs still cannot be controlled independently. A more attractive solution is then proposed in [14–19]. It is observed that TZs can be generated and independently controlled without any cross-coupled or extracted-pole structures. As a result, the derived network only involves resonators serially cascaded one after another, providing the simplest configuration for high selectivity filters. In [18], second and third-order in-line filters are theoretically discussed by separately analyzing the capacitive and inductive couplings of each mixed-coupled structure. Nevertheless, this mechanism requires a number of manipulations and a general approach for in-line filters with higher orders and more

frequency variant couplings are still unsolved. Recently, a favorable direct synthesis method is reported in [19], but is available for a very particular in-line condition where only one TZ can be realized. Lacking a general direct synthesis approach, whether a selected in-line network can realize required frequency response is still not predictable. In [20], a general direct synthesis approach is presented for synthesizing in-line filters with multiple TZs for the first time. However, there are some limitations in [20]. First, it must consider both the couplings and capacitances of a traditional low-pass prototype. Second, it needs to use similar transformation, and it cannot implement the adjacent FVCs. Third, the number of Tzs implemented by [20] is half of the filter order.

In this paper, an improved matrix synthesis approach for inline filter is presented. Compared with the conventional synthesis approach for inline topology filter [20], the method presented in this paper has following advantages: First, it is unnecessary to consider both the couplings and capacitances of a traditional low-pass prototype. Second, there is no need to use similar transformation, and the adjacent FVC can be implemented. Third, the approach presented can implement more finite transmission zeros than the previous works. The maximum number of TZs can be increased to $N-1$. With the source load coupling, the maximum number of TZs can be as many as the filter order N.

In the following, the basic theory of the synthesis technique for inline filter is detailed in Section 2. In Section 3, two examples with different topologies and specifications are synthesized to show the validation of the method presented in this paper. A conclusion is provided in Section 4.

2. BASIC THEORY

Generally, the topology of inline filter is shown in Fig. 1. The transmission coefficient S_{21} and reflection coefficient S_{11} of a inline filter network can be described as a ratio of two polynomials [3]:

$$S_{21}(s) = \frac{P(s)}{\varepsilon E(s)} \qquad S_{11}(s) = \frac{F(s)}{\varepsilon_R E(s)} \tag{1}$$

where $s = j\omega$ is a complex frequency variable, and ε and ε_R are ripple constants related to the maximum return loss. Polynomial $P(s)$ is determined from finite transmission zeros. Once N, the passband return loss and the transmission zeros p_i are given, polynomial $F(s)$ can be calculated using a recursion formula [3]. From the conservation of energy, the relation between numerator polynomials and denominator polynomials can be expressed as

$$E(s)E(s)^* = \frac{F(s)F(s)^*}{\varepsilon_R^2} + \frac{P(s)P(s)^*}{\varepsilon^2} \tag{2}$$

where superscript * denotes the complex conjugate, $\varepsilon_R = 1$ when the degree of $F(s)$ is greater than that of $P(s)$. If $F(s)$ and $P(s)$ have the same degree,

$$\varepsilon_R = \varepsilon \Big/ \sqrt{\varepsilon^2 - 1} \tag{3}$$

S-parameters can also be directly related to the coupling coefficients as follows:

$$S_{21} = -2j\left[A^{-1}\right]_{N+2,1} \qquad S_{11} = 1 + 2j\left[A^{-1}\right]_{1,1} \tag{4}$$

where matrix A is given by

$$A = -jR + \omega \cdot C + M + \omega \cdot M_1 \tag{5}$$

ω is the normalized frequency; C represents the capacitance matrix; and C is a unit matrix except $C_{11} = C_{N+2,N+2} = 0$, R a $(N+2)^*(N+2)$ matrix whose only nonzero entries are $R_{11} = R_{N+2,N+2} = 1$, M the $(N+2)^*(N+2)$ coupling matrix, and M_1 the $(N+2)^*(N+2)$ frequency variant coupling matrix.

At this point, the synthesis problem can be formulated simply: determine the coupling matrix M and frequency variant coupling matrix M_1 such that the scattering parameters given by Eq. (4) reproduce the insertion and return loss given by the prototype.

We propose to solve this problem by optimization for the following reasons.

1) We can strictly enforce the desired topology, such as adjacent FVCs, which cannot be implemented by analysis synthesis technique.
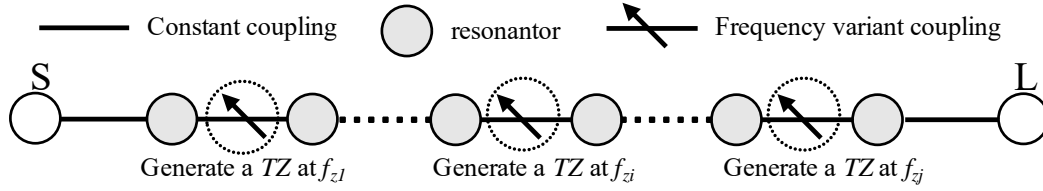
Figure 1. General topology of inline filters.

2) We can constrain specific coupling elements to be of a given sign or within a magnitude range if intended implementation calls for such a constraint.

Keeping in mind that the filtering functions under consideration are rational functions of frequency, they are uniquely specified by the location of their poles and zeros and an additional scaling constant. Since the zeros of the filtering function are identical to those of S_{11}, and its poles coincide with the zeros of S_{21}, the original analytic structure is recovered from the vanishing of S_{11} and S_{21} at the corresponding frequency points. To determine the scaling constant, we evaluate the return loss at $\omega' = \pm 1$ to get $|S_{11}(\omega' = \pm 1)| = (\varepsilon/\sqrt{1 + \varepsilon^2})$. Consequently, the following cost function is used in this work

$$\cos tfun = \sum_{i=1}^{N} |S_{11}(p_i)|^2 + \sum_{i=1}^{Nz} |S_{21}(z_i)|^2 + \left(|S_{11}(s_{pi} = \pm j)| - \frac{\varepsilon}{\sqrt{1 + \varepsilon^2}} \right)^2 \tag{6}$$

Here, p_i is the reflection the zeros, and z_i represents the TZs. By minimizing the cost function in Eq. (6), the nonzero coupling matrix elements M_{pq} of the "$N + 2$" coupling matrix M and the element M_{1pq} frequency variant coupling matrix M_1 can be obtained by a optimization method. The process of the synthesis technique in this paper consists of Solvopt algorithm [21] for a local optimizer and genetic algorithm [22] for a global optimizer, respectively. The optimization flowchart is shown in Fig. 2. The Solvopt algorithm can use the user-supplied gradients or not. Using the user-supplied gradients can accelerate the optimization efficiency. The gradients of cost function in Eq. (6) are given in Equation (7).

$$\frac{\partial S_{11}}{\partial M_{pq}} = -4jP_{pq} \left[A^{-1} \right]_{1p} \left[A^{-1} \right]_{q1}, \quad p \neq q \tag{7a}$$

$$\frac{\partial S_{11}}{\partial M_{1pq}} = -4j\omega P_{1pq} \left[A^{-1} \right]_{1p} \left[A^{-1} \right]_{q1}, \quad p \neq q \tag{7b}$$

$$\frac{\partial S_{11}}{\partial M_{pp}} = -2jP_{pp} \left[A^{-1} \right]_{1p} \left[A^{-1} \right]_{p1}, \quad p = q \tag{7c}$$

$$\frac{\partial S_{21}}{\partial M_{pq}} = 2jP_{pq} \left(\left[A^{-1} \right]_{n+2,p} \left[A^{-1} \right]_{q1} + \left[A^{-1} \right]_{n+2,q} \left[A^{-1} \right]_{p1} \right) \quad p \neq q \tag{7d}$$

$$\frac{\partial S_{21}}{\partial M_{1pq}} = 2j\omega P_{1pq} \left(\left[A^{-1} \right]_{n+2,p} \left[A^{-1} \right]_{q1} + \left[A^{-1} \right]_{n+2,q} \left[A^{-1} \right]_{p1} \right) \quad p \neq q \tag{7e}$$

$$\frac{\partial S_{21}}{\partial M_{pp}} = 2jP_{pp} \left[A^{-1} \right]_{n+2,p} \left[A^{-1} \right]_{p1}, \quad p = q \tag{7f}$$

3. EXPERIMENT RESULTS

For verification of the synthesis method described above, two examples are tested in this section. Each of them is characterized by a different topology scheme and number of transmission zeros. In all presented examples, the algorithm begins by generating random numbers for non-zero elements of the coupling matrix, whose values lie within specified limits $[-10, 10]$. The process will terminate until the value of the cost function drops below 10^{-12}.
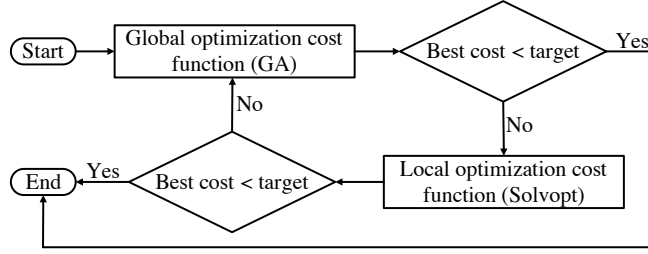
Figure 2. Optimization flowchart of the method presented in this paper.
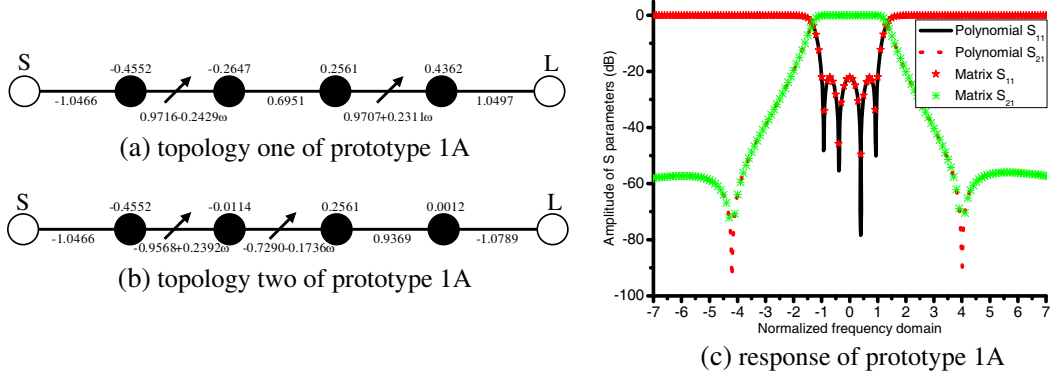

(a) topology one of prototype 1A

(b) topology two of prototype 1A

(c) response of prototype 1A

Figure 3. Topology and response of prototype 1A.

(a) topology of prototype 1B
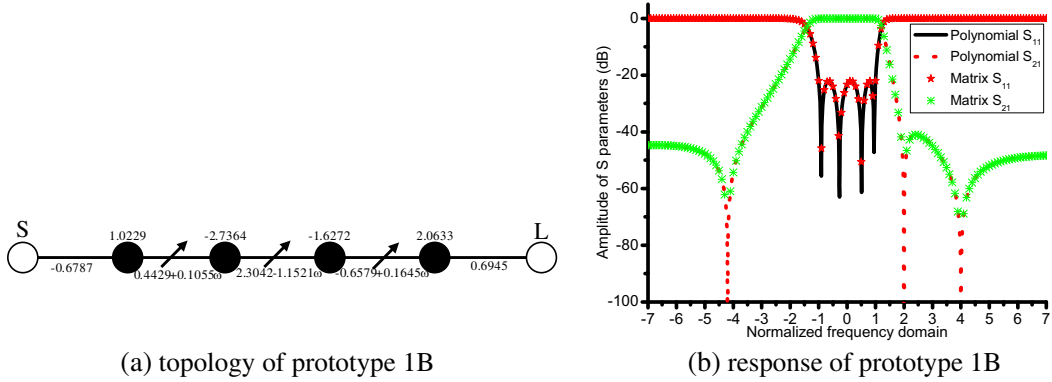
(b) response of prototype 1B

Figure 4. Topology and response of prototype 1B.

3.1. Example One

The first synthesized inline filter example is a fourth-order 22-dB return loss with different TZs numbers. Other specifications are shown as following:

Prototype 1A: There are two TZs located at $-4.2j$ and $4j$, and the topologies are shown as in Fig. 3(a) and Fig. 3(b).

Prototype 1B: There are three TZs located at $-4.2j$, $4j$ and $2j$, and the topologies are shown as in Fig. 4(a).

Prototype 1C: There are four TZs located at $-4.2j$, $4j$, $2j$ and $-2.3j$, and the topologies are shown as in Fig. 5(a).

Using the method presented in Section 2, we obtain the coupling coefficients. The values of the cost function for prototype 1 are 1.6205e-13, 9.3226e-15, 1.3930e-13, 5.0382e-13, respectively. All the values are less than 10^{-12}. In order to show the details of the novelty, we will give clear mathematical

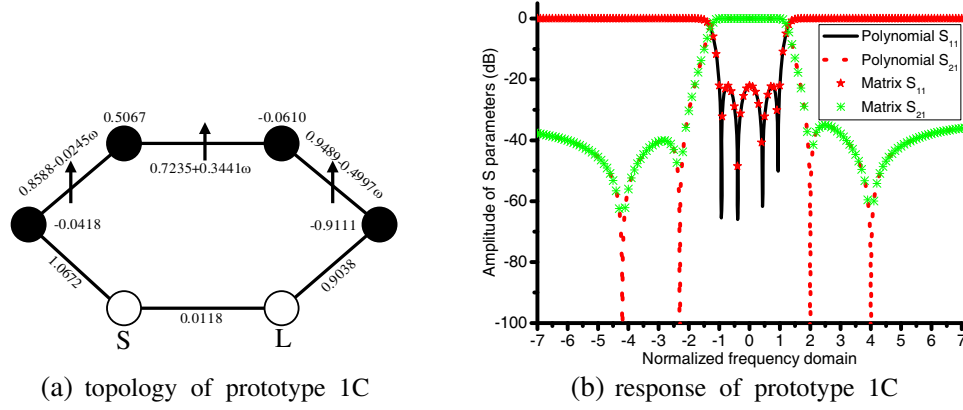(a) topology of prototype 1C   (b) response of prototype 1C

Figure 5. Topology and response of prototype 1C.

derivations and results of prototype 1C. For prototype 1C, the topology of coupling matrix M is M_topo, and FVC coupling matrix M_1 is M_1_topo, which is given as

$$M\_topo = \begin{bmatrix} 0 & 1 & 0 & 0 & 0 & 0 \\ 1 & 1 & 1 & 0 & 0 & 0 \\ 0 & 1 & 1 & 1 & 0 & 0 \\ 0 & 0 & 1 & 1 & 1 & 0 \\ 0 & 0 & 0 & 1 & 1 & 1 \\ 0 & 0 & 0 & 0 & 1 & 0 \end{bmatrix} \tag{8a}$$

$$M_1\_topo = \begin{bmatrix} 0 & 0 & 0 & 0 & 0 & 0 \\ 0 & 0 & 1 & 0 & 0 & 0 \\ 0 & 1 & 0 & 1 & 0 & 0 \\ 0 & 0 & 1 & 0 & 1 & 0 \\ 0 & 0 & 0 & 1 & 0 & 0 \\ 0 & 0 & 0 & 0 & 0 & 0 \end{bmatrix} \tag{8b}$$

In Equation (8), the coupling between two resonators is denoted by 1. If there is no coupling between two resonators, the element of the matrix is denoted by 0. Then we use GA to optimize the cost function, Equation (6), and coupling matrices M and M_1 are obtained as

$$M = \begin{bmatrix} 0 & 2.2293 & 0 & 0 & 0 & 1.5311 \\ 2.2293 & 0.7977 & 2.9994 & 0 & 0 & 0 \\ 0 & 2.9994 & 0.6284 & -0.8798 & 0 & 0 \\ 0 & 0 & -0.8798 & -0.1575 & 2.0438 & 0 \\ 0 & 0 & 0 & 2.0438 & -1.8739 & 1.1295 \\ 1.5311 & 0 & 0 & 0 & 1.1295 & 0 \end{bmatrix} \tag{9a}$$

$$M_1 = \begin{bmatrix} 0 & 0 & 0 & 0 & 0 & 0 \\ 0 & 0 & 0.2834 & 0 & 0 & 0 \\ 0 & 0.2834 & 0 & 0.2469 & 0 & 0 \\ 0 & 0 & 0.2469 & 0 & -1.2106 & 0 \\ 0 & 0 & 0 & -1.2106 & 0 & 0 \\ 0 & 0 & 0 & 0 & 0 & 0 \end{bmatrix} \tag{9b}$$

The value of cost function in Eq. (6) is 0.6556. Finally, we use Solvopt to optimize the cost function, Equation (6), and coupling matrices M and M_1 are obtained as

$$M = \begin{bmatrix} 0 & 1.0672 & 0 & 0 & 0 & 0.0118 \\ 1.0672 & -0.0418 & 0.8586 & 0 & 0 & 0 \\ 0 & 0.8586 & 0.5067 & 0.7235 & 0 & 0 \\ 0 & 0 & 0.7235 & -0.0610 & 0.9489 & 0 \\ 0 & 0 & 0 & 0.9489 & -0.9111 & 0.9038 \\ 0.0118 & 0 & 0 & 0 & 0.9038 & 0 \end{bmatrix} \tag{10a}$$

$$M_1 = \begin{bmatrix} 0 & 0 & 0 & 0 & 0 & 0 \\ 0 & 0 & -0.0245 & 0 & 0 & 0 \\ 0 & -0.0245 & 0 & 0.3441 & 0 & 0 \\ 0 & 0 & 0.3441 & 0 & -0.4997 & 0 \\ 0 & 0 & 0 & -0.4997 & 0 & 0 \\ 0 & 0 & 0 & 0 & 0 & 0 \end{bmatrix} \tag{10b}$$

The value of cost function in Eq. (6) is 5.0382e-13.

For prototype 1A, the coupling coefficients are shown in Fig. 3(a) and Fig. 3(b), and the response is shown in Fig. 3(c). For prototype 1B, the coupling coefficients are shown in Fig. 4(a), and the response is shown in Fig. 4(b). For prototype 1C, the coupling coefficients are shown in Fig. 5(a), and the response is shown in Fig. 5(b). The polynomials response and matrix response agree well. From Fig. 3(b) Fig. 4(a), we can see that the adjacent FVCs can be implemented by the method presented in this paper. The adjacent FVCs cannot be implemented by the method in [20]. From Fig. 5(a), we can see that the number of TZs can be as many as the filter order with the source load couplings.

3.2. Example Two

The second synthesized inline filter example is a fifth-order with 22-dB return loss with different TZs numbers. Other specifications are shown as follows:

Prototype 2A: There are two TZs located at $-4.2j$ and $4j$, and the topologies are shown as in Fig. 6(a).

Prototype 2B: There are three TZs located at $-4.2j$, $4j$ and $2j$, and the topologies are shown as in Fig. 7(a) and Fig. 7(b).

Prototype 2C: There are four TZs located at $-4.2j$, $4j$, $2j$ and $-2.3j$, and the topologies are shown as in Fig. 8(a).

Prototype 2D: There are five TZs Located at $-4.2j$, $4j$, $2j$, $-2.3j$ and $6.1j$, and the topologies are shown as in Fig. 9(a).

Using the method presented in Section 2, we obtain the coupling coefficients. The values of the cost function for prototype 2 are 1.2108e-14, 8.4215e-14, 2.0161e-13, 6.6074e-14, 2.5238e-13, respectively. All the values are less than 10^{-12}. For prototype 2A, the coupling coefficients are shown in Fig. 6(a), and the response is shown in Fig. 3(b). For prototype 2B, the coupling coefficients are shown in Fig. 7(a) and Fig. 7(b), and the response is shown in Fig. 7(c). For prototype 2C, the coupling coefficients are shown in Fig. 8(a), and the response is shown in Fig. 8(b). For prototype 2D, the coupling coefficients are shown in Fig. 9(a), and the response is shown in Fig. 9(b). The polynomials response and matrix response agree well. From Fig. 7(b) and Fig. 8(a), we can see that the adjacent FVCs can be implemented by the method presented in this paper. The adjacent FVCs cannot be implemented by the method in [20]. From Fig. 9(a), we can see that the number of TZs can be as many as the filter order with the source load couplings. In order to show the advantage, we add the tabular form in Table 1.
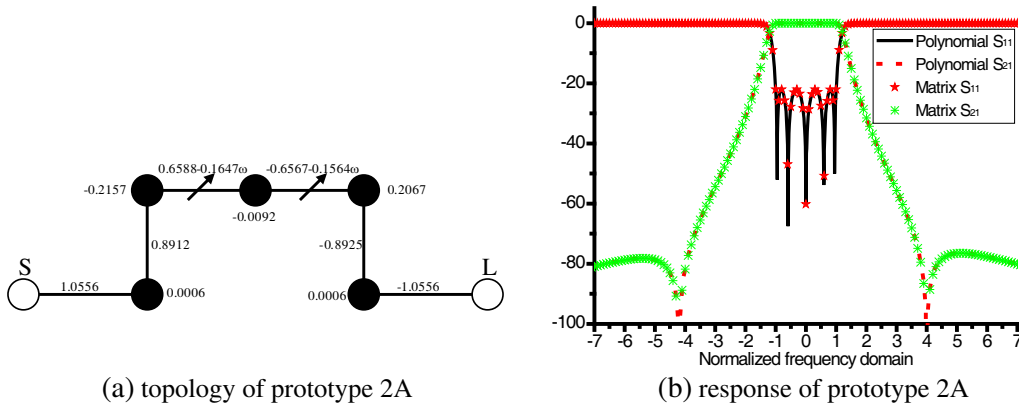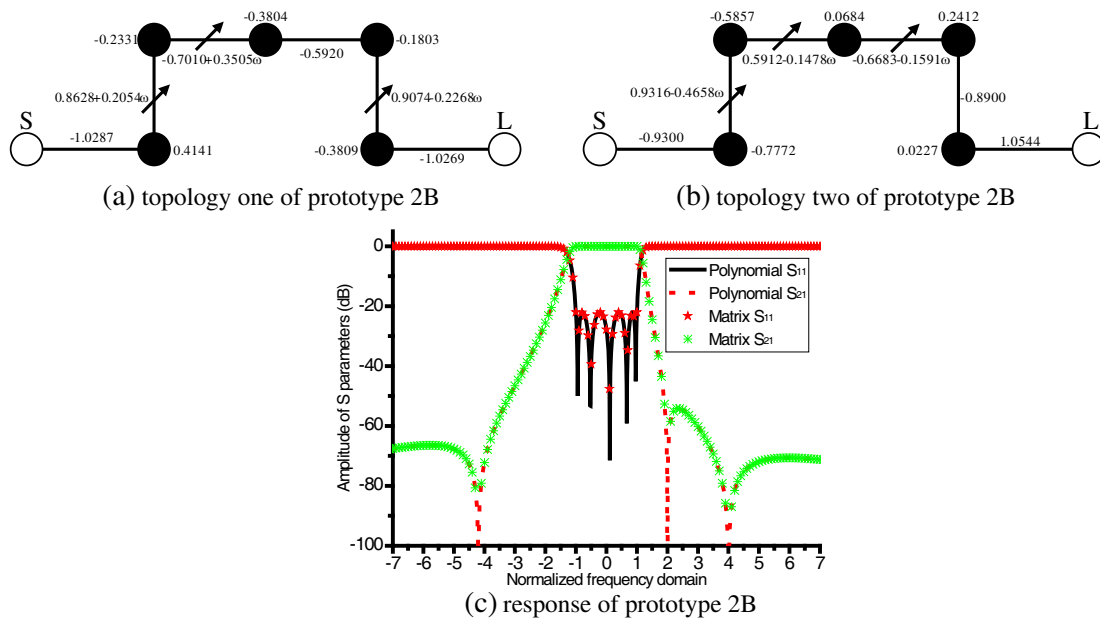

(a) topology of prototype 2A

(b) response of prototype 2A

Figure 6. Topology and response of prototype 2A.

(a) topology one of prototype 2B

(b) topology two of prototype 2B

(c) response of prototype 2B

Figure 7. Topology and response of prototype 2B.

(a) topology of prototype 2C

(b) response of prototype 2C

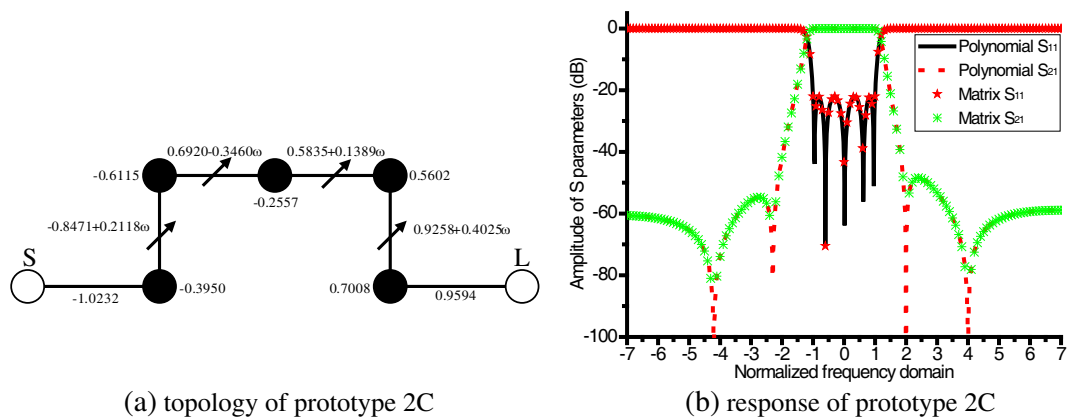**Figure 8.** Topology and response of prototype 2C.

(a) topology of prototype 2D
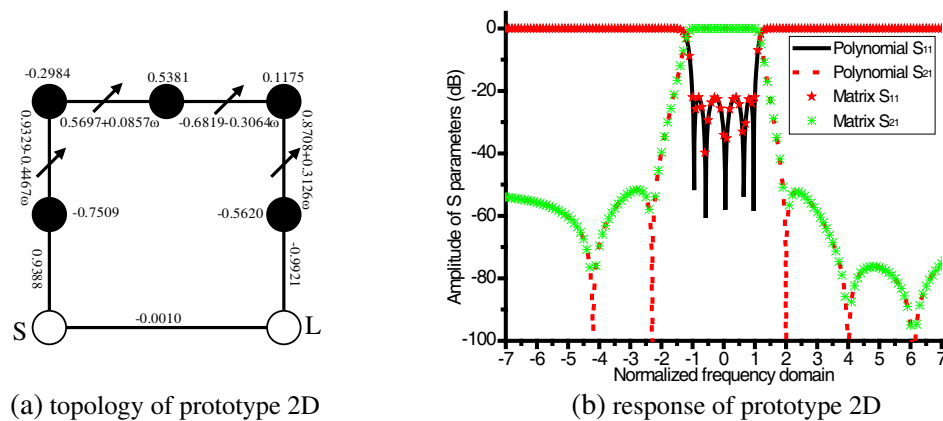
(b) response of prototype 2D

Figure 9. Topology and response of prototype 2D.

Table 1. Comparison of Reference [20] and this paper.

Maximun number of ftzs	Example one	Example two
Reference [20]	2 ftzs	2 ftzs
This paper	4 ftzs	5 ftzs

4. CONCLUSION

An improved matrix synthesis approach for inline filter is presented in this paper. Frequency-variant couplings (FVC) can generate and control multiple finite transmission zeros (TZs). Compared with the conventional synthesis method for inline topology filters, the method presented in this paper has following advantages: First, it is unnecessary to consider both the couplings and capacitances of a traditional low-pass prototype. Second, there is no need to use similar transformation, and the adjacent FVCs can be implemented. Third, the approach presented can implement more TZs than the previous works. The maximum number of TZs can be as many as the filter order with the source-load coupling. Two examples with different topologies and specifications are synthesized to show the validation of the method presented in this paper.

ACKNOWLEDGMENT

REFERENCES

1. Atia, A., A. Williams, and R. Newcomb, "Narrow-band multiplecoupled cavity synthesis," *IEEE Trans. Circuits Syst.*, Vol. 21, No. 5, 649–655, Sep. 1974.

2. Cameron, R. J., "General coupling matrix synthesis methods for Chebyshev filtering functions," *IEEE Trans. Microw. Theory Techn.*, Vol. 47, No. 4, 433–442, Apr. 1999.

3. Cameron, R. J., "Advanced coupling matrix synthesis techniques for microwave filters," *IEEE Trans. Microw. Theory Techn.*, Vol. 51, No. 1, 1–10, Jan. 2003.

4. Cameron, R. J., "Advanced coupling matrix synthesis techniques for microwave filters," *IEEE Trans. Microw. Theory Techn.*, Vol. 51, No. 1, 1–10, Jan. 2003.

5. Kozakowski, P., A. Lamecki, P. Sypek, and M. Mrozowski, "Eigenvalue approach to synthesis of prototype filters with source/load coupling," *IEEE Microw. Wireless Compon. Lett.*, Vol. 15, No. 2, 98–100, Feb. 2005.

6. Cameron, R. J., C. Kudsia, and R. Mansour, "Coupling matrix synthesis of filter networks," *Microwave Filters for Communication Systems*, 1st edition, Wiley, Hoboken, NJ, USA, 2007.

7. Amari, S. and U. Rosenberg, "Synthesis and design of novel in-line filters with one or two real transmission zeros," *IEEE Trans. Microw. Theory Techn.*, Vol. 52, No. 5, 1464–1478, May 2004.

8. Amari, S. and G. Macchiarella, "Synthesis of inline filters with arbitrarily placed attenuation poles by using nonresonating nodes," *IEEE Trans. Microw. Theory Techn.*, Vol. 53, No. 10, 3075–3081, Oct. 2005.

9. Macchiarella, G. and S. Tamiazzo, "Synthesis of microwave duplexers using fully canonical microstrip filters," *IEEE MTT-S Int. Microw. Symp. Dig.*, 721–724, Jun. 2009.

10. Glubokov, O. and D. Budimir, "Extraction of generalized coupling coefficients for inline extracted pole filters with nonresonating nodes," *IEEE Trans. Microw. Theory Techn.*, Vol. 59, No. 12, 3023–3029, Dec. 2011.

11. Zhao, P. and K.-L. Wu, "A direct synthesis approach of bandpass filters with extracted-poles," *Proc. Asia-Pacific Microw. Conf.*, 25–27, Seoul, South Korea, Nov. 2013.

12. Wang, Y. and M. Yu, "True inline cross-coupled coaxial cavity filters," *IEEE Trans. Microw. Theory Techn.*, Vol. 57, No. 12, 2958–2965, Dec. 2009.

13. Bastioli, S. and R. V. Snyder, "Inline pseudoelliptic TM01δ-mode dielectric resonator filters using multiple evanescent modes to selectively bypass orthogonal resonators," *IEEE Trans. Microw. Theory Techn.*, Vol. 60, No. 12, 3988–4001, Dec. 2012.

14. Amari, S., M. Bekheit, and F. Seyfert, "Notes on bandpass filters whose inter-resonator coupling coefficients are linear functions of frequency," *IEEE MTT-S Int. Microw. Symp. Dig.*, 1207–1210, Atlanta, GA, USA, Jun. 2008.

15. Amari, S. and J. Bornemann, "Using frequency-dependent coupling to generate finite attenuation poles in direct-coupled resonator bandpass filters," *IEEE Microw. Guided Wave Lett.*, Vol. 9, No. 10, 404–406, Oct. 1999.

16. Politi, M. and A. Fossati, "Direct coupled waveguide filters with generalized Chebyshev response by resonating coupling structures," *Proc. Eur. Microw. Conf. (EuMC)*, 966–969, Sep. 2010.

17. Rosenberg, U., S. Amari, and F. Seyfert, "Pseudo-elliptic direct-coupled resonator filters based on transmission-zero-generating irises," *Proc. Eur. Microw. Conf. (EuMC)*, 962–965, Sep. 2010.

18. Wang, H. and Q.-X. Chu, "An inline coaxial quasi-elliptic filter with controllable mixed electric and magnetic coupling," *IEEE Trans. Microw. Theory Techn.*, Vol. 57, No. 3, 667–673, Mar. 2009.

19. Tamiazzo, S. and G. Macchiarella, "Synthesis of cross-coupled filters with frequency-dependent couplings," *IEEE Trans. Microw. Theory Techn.*, Vol. 65, No. 3, 775–782, Mar. 2017.

20. He, Y., G. Macchiarella, G. Wang, W. Wu, L. Sun, L. Wang, and R. Zhang, "A direct matrix synthesis for in-line filters with transmission zeros generated by frequency-variant couplings," *IEEE Trans. Microw. Theory Techn.*, Vol. 66, No. 6, 1780–1789, Apr. 2018.

21. SolvOpt manual and SolvOpt Toolbox for matlab, Available: http://www.kfunigraz.ac.at/imawww/kuntsevich/solvopt/index.html.

22. GA Toolbox, http://www.shef.ac.uk/acse/research/ecrg/getgat.html.